Insulator-Metal Phase Diagram of the Optimally Doped Manganites from the Disordered Holstein-Double Exchange Model

Sanjeev Kumar* and Pinaki Majumdar
Harish-Chandra Research Institute,
Chhatnag Road, Jhusi, Allahabad 211 019, India
(Oct 24, 2005)

We study the Holstein-Double Exchange model in three dimensions in the presence of substitutional disorder. Using a new Monte Carlo technique we establish the phase diagram of the clean model and then focus on the effect of varying electron-phonon coupling and disorder at fixed electron density. We demonstrate how extrinsic disorder controls the interplay of lattice polaron effects and spin fluctuations and leads to widely varying regimes in transport. Our results on the disorder dependence of the ferromagnetic T_c and metal-insulator transitions bear direct comparison to data on the 'optimally doped', $x = 0.3-0.4$, manganites. We highlight disorder induced polaron formation as a key effect in these materials, organise a wide variety of data into a simple 'global phase diagram', and make several experimental predictions.

The Holstein-Double Exchange (H-DE) model provides a minimal description of strongly coupled charge, spin, and lattice degrees of freedom, typical of the perovskite manganites $A_{1-x}A'_xMnO_3$ [1], and captures the interplay of polaronic tendency and spin disorder that occurs in these materials. Although a detailed solution has not been available in three dimensions (3D), the H-DE model is believed to describe the trend towards stronger localisation and weakened ferromagnetism observed with reducing A site ionic radius (r_A) in the manganites.

The role of quenched disorder in these systems, arising, for example, from the cation size mismatch (σ_A) is only partially understood. Most of the disorder related theory [2,3] has focused on effects near a first order phase boundary, *i.e*, the 'bicritical' region [4], motivated by the observation of cluster coexistence in some materials [5]. Phase competetion and bicriticality, however, occurs only in a limited part of the phase diagram. Studies with controlled variation in σ_A indicate that quenched disorder has a dramatic effect on the ferromagnetic T_c and resistivity [6–9], and optical response [10] even far from bicriticality. The origin of these effects remain unexplained.

Our primary contribution in this paper is to demonstrate how this unusual sensitivity arises due to a positive feedback of quenched disorder on the polaron formation tendency, and its interplay with spin fluctuations. Through a detailed real space solution of the disordered H-DE model on large 3D lattices we (*i*) demonstrate disorder controlled metal-insulator transitions (MIT), in the ground state and at finite temperature, that are absent in the 'clean' system, (*ii*) explain the rapid suppression of T_c with increasing disorder, (*iii*) compare our results in detail with data on the manganites at $x = 0.3 - 0.4$, constructing a 'global phase diagram', and (*iv*) make testable predictions about the σ_A dependence of optical spectral weight, lattice distortion, and tunneling density of states in the optimally doped manganites.

We study the adiabatic disordered (*d*) H-DE model:

$$H = -t \sum_{\langle ij \rangle \sigma} (\ c^\dagger_{i\sigma} c_{j\sigma} \ + \ h.c \ ) + \sum_i (\epsilon_i - \mu) n_i - \lambda \sum_i n_i x_i - J_H \sum_i \mathbf{S}_i . \sigma_i + \frac{K}{2} \sum_i x_i^2 \quad (1)$$

The t are nearest neighbour hopping on a cubic lattice, ϵ_i is the quenched binary disorder, with $\bar{\epsilon}_i = 0$ and value $\pm\Delta$, λ is the electron-phonon (EP) interaction, coupling electron density to the local distortion x_i, K is the stiffness, μ is the chemical potential, and J_H is the Hunds coupling. The parameters in the problem are λ/t, Δ/t, electron density n, and temperature T. We treat the phonons and spins as classical (the adiabatic limit), assume $J_H/t \to \infty$, and set $|\mathbf{S}| = 1$. We also set $K = 1$ and measure energy, frequency, T, *etc*, in units of t.

The clean H-DE model was proposed early on [11] as a minimal model for the manganites, and a mean field study [11] suggested strong decrease of T_c and increasing localisation with increase in EP coupling. More recently the H-DE model with 'cooperative phonons' has been analysed [12] in 3D, yielding a thermally driven MIT at low n but not near optimality. The effect of disorder has been considered on EP-DE models but with focus mainly on phase coexistence [13] and bicriticality [3]. These studies yield insight on how disorder leads to cluster formation near a first order phase boundary [2,13], or its impact on a commensurate charge ordered phase [3], but do not have much bearing on the effects observed, for example, at $x = 0.3$, where there is no obvious phase competetion. In our understanding, the effects of disorder in the manganites, away from bicriticality, await an explanation. In this paper we overcome a key technical limitation of the earlier studies and provide new results on transport combining the effects of strong EP coupling, thermal spin fluctuations, and quenched disorder, on lattices upto 12^3 in size.

Since we work with $J_H/t \to \infty$, the electron spin is 'slaved' to the core spin orientation leading to an effectively spinless, hopping disordered model: $H = -\sum_{\langle ij \rangle}(t_{ij}\gamma_i^\dagger\gamma_j + h.c\,) + \sum_i(\epsilon_i - \mu - \lambda x_i)n_i + (K/2)\sum_i x_i^2$. The hopping amplitude depends on the spin orientations via $t_{ij}/t = cos\frac{\theta_i}{2}cos\frac{\theta_j}{2} + sin\frac{\theta_i}{2}sin\frac{\theta_j}{2}e^{i(\phi_i - \phi_j)}$, where θ_i and ϕ_i are respectively the polar and azimuthal angles of the spin $\mathbf{S}_i$. We use our recently developed "travelling cluster approximation" (TCA) [14] for solving the annealing problem on large lattices, by computing the energy cost of a MC update by constructing a 'cluster Hamiltonian', of $N_c = L_c^3$ sites, around the update site. We will use $N_c = 4^3$ and, as documented earlier [14], this is sufficient for equilibriating the spin and lattice variables. The electronic properties, *e.g*, resistivity, density of states, and optical response, are obtained by diagonalising the *full* electron Hamiltonian on the equilibrium $\{x_i, \mathbf{S}_i\}$ configurations, averaging thermally and finally over $8-10$ realisations of disorder $\{\epsilon_i\}$. The transport results are obtained using a formulation described in detail previously [15]. We will use system size $N = 8^3$, but have checked our results on N upto 12^3. Our resistivity results are in units of $\hbar a_0/(\pi e^2)$, where a_0 is the lattice spacing. As a rough estimate, $\rho = 1$ in our units would correspond to $\sim 30\mu\Omega$cm.

Let us summarise the phases of the clean H-DE model before addressing the effects of disorder. (**a**). Structurally, a phase can be either charge ordered (CO), or charge disordered, *i.e* a polaron liquid (PL), or homogeneous, *i.e* a Fermi liquid (FL). (**b**). Magnetically it can be either ferromagnetic (F) or paramagnetic (P), and (**c**). in terms of electrical response it can be a 'metal', with $d\rho/dT > 0$, or an insulator, with $d\rho/dT < 0$.

Combining these features, the ground state can be either a ferromagnetic Fermi liquid (F-FL), or F-PL, or F-CO, depending on λ and n, while finite T allows P-FL, P-PL, and P-CO phases as well. Notice that while the threshold for *single polaron* trapping, *i.e* $n = 0$, in 3D, is $E_p = \lambda^2/2K \approx 5.4t$, *i.e* $\lambda_c(n=0) \sim 3.3$ [16], at *finite density* the threshold for a collective PL is lower, *e.g*, $\lambda_c(n = 0.3) \sim 2.6$. These thresholds are further affected

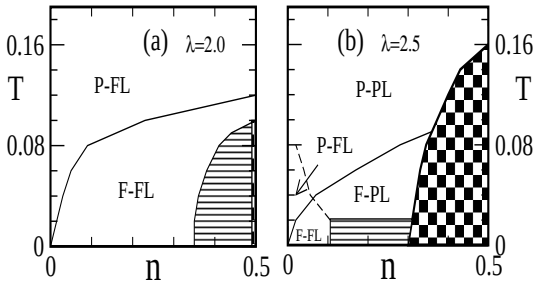

FIG. 1. Phase diagram in the clean problem: (a) and (b) show the phase diagram at $\lambda = 2.0$ and $\lambda = 2.5$ respectively. The notation for the phases is explained in the text. The chessboard pattern is for a charge ordered (CO) phase with (π, π, π) modulation. Shaded regions represent coexistence.

by structural and spin disorder.

For $\lambda \lesssim 2.0$, Fig.1.(a), the phases are (i) F-FL at low T away from $n = 0.5$, (ii) P-FL at high T, and (iii) a F-CO phase at $n = 0.5$, separated from the F-FL, at low T, by a window of phase separation. For $\lambda = 2.0$ the T_c at $n = 0.5$ is suppressed with respect to the pure DE problem, but is still larger than the CO scale T_{CO}. At stronger coupling, of which $\lambda = 2.5$ is typical, Fig.1.(b)., much of the phase diagram is taken up by insulating phases. As λ is increased beyond 2.5 the metallic window at low n shrinks quickly and all the phases turn insulating. The ground state, however, continues to be ferromagnetic since we have not included any competing antiferromagnetism (AF). From the resistivity we confirmed that the clean model does not show a thermally driven MIT except for $n \lesssim 0.1$, as noted earlier [12].

Even weak structural disorder dramatically affects the electronic state at strong coupling, leading to metal-insulator transitions which are not present in the clean limit. In the rest of the paper we focus on $n = 0.3$, typical of the high density metallic regime, and study the effect of varying disorder and EP coupling. Since the r_A controlled bandwidth variation in real materials is relatively small we use only a $\pm 10\%$ variation in λ/t about $\lambda = 2.0$ and study the weak disorder regime, $\Delta = 0 - 1.0$.

Disorder creates density inhomogeneities in the FL which are amplified by the EP coupling, leading to a rapid rise in residual resistivity, and also opens up a window for the crucial F-FL to P-PL crossover. Fig.2.$(a) - (c)$ show $\rho(T)$ with varying λ and Δ illustrating the three broad transport regimes. At $\lambda = 1.8$, which is towards the lower end of our coupling range, moderate Δ increases $\rho(0)$ but the overall $\rho(T)$ has the same nature as in the simple DE model [15] and neither EP coupling nor disorder seems to have any qualitative effect. This is true of $\Delta \lesssim 0.6$ and, we suggest, is akin to what one observes in $La_{0.7}Sr_{0.3}MnO_3$. At $\Delta = 1.0$, where $\rho(0) \gtrsim 100 \sim \rho_{Mott}$ we see hints of a weak downturn in $\rho(T)$ at high T. Overall, $\rho(T)$ at $\lambda = 1.8$ is mainly characterised by a F-FL to P-FL crossover. The density of states (DOS), Fig.2.(d), remains featureless at all T and the lattice distortions, Fig.2.(g), are weak with no significant variation across T_c. This "DE like" character in $\rho(T)$ survives upto $\lambda = 2.2$ in the clean limit, see Fig.2.$(b) - (c)$. However, for $\lambda \gtrsim 2.0$ addition of weak disorder (i) sharply increases $\rho(0)$ and creates a pseudogap in the DOS, (ii) maintains a regime with $d\rho/dT > 0$ for $T \lesssim T_c$, but (iii) crosses over to an 'insulating' PL regime with $d\rho/dT < 0$ for $T \gtrsim T_c$. As Fig.2.$(h) - (i)$ indicate, these changes are associated with large lattice distortions and their variation across T_c. For $\Delta \sim 1.0$ the ground state itself turns insulating for $\lambda \gtrsim 2.0$. We provide a compact picture of the various MIT in Fig.3, discussed later.

To gain insight on the F-FL to P-PL crossover we also calculated the 'effective carrier number', $n_{eff}(\bar{\omega}, T) =$

$\int_0^{\bar{\omega}} \sigma(\omega,T)d\omega$, at $T=0$ and $\bar{\omega}=0.5$, as well the density field $n(\mathbf{r},T)$. The combination of n_{eff}, Fig.4.(a), the spatial patterns (not shown here) and the DOS, Fig.2.(e), suggest the following scenario at strong coupling and moderate disorder: (i) there is polaronic localisation of a *fraction* of carriers (states at $\omega<\mu$) at $T=0$, lowering n_{eff}, but the states at the chemical potential remain extended, (ii) the polaronic states are further localised with increasing T due to DE spin disorder, while the delocalised electrons near μ experience scattering from the spin fluctuations, leading to $d\rho/dT>0$, (iii) by the time $T\sim T_c$ the net disorder arising from ϵ_i, the lattice distortions, and spin disorder is so large that the system is effectively at a localisation transition on the complex $\{\epsilon_i, x_i, \mathbf{S}_i\}$ background: the states at μ also get localised, (iv) the $T\gtrsim T_c$ phase has a modest 'mobility gap' (at moderate λ,Δ) so there is no simple activated behaviour. The pseudogap in the DOS, Fig.2.(e), *deepens* initially and gradually fills up for $T\gtrsim T_c$.

Let us consider the relevance of these results to manganites at $x\sim 0.3-0.4$, away from commensurate filling and charge ordering instabilities. The mean hopping amplitude between Mn ions, via the oxygen orbitals, is controlled by r_A through the Mn-O-Mn bond angle. The mismatch between different A site cations is quantified through the variance, σ_A, of the ionic size, and acts as

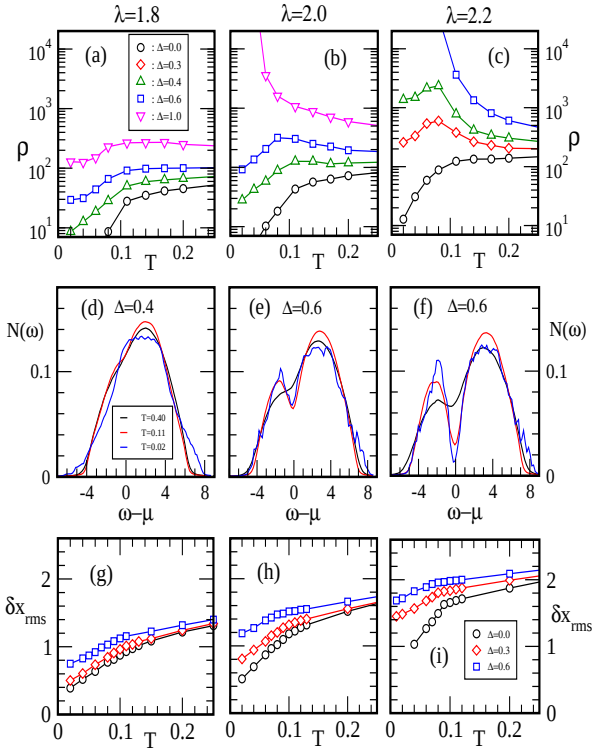

FIG. 2. Colour online: Resistivity, $\rho(T)$, DOS, and lattice distortion at $n=0.3$. $(a)-(c)$. $\rho(T)$, with varying λ and Δ. $(d)-(f)$. DOS, $N(\omega,T)$ for the indicated parameters. $(g)-(i)$. RMS lattice distortion, $\delta x_{rms}=\sqrt{\langle(x_i-\bar{x})^2\rangle}$, where $\bar{x}$ is the system averaged distortion.

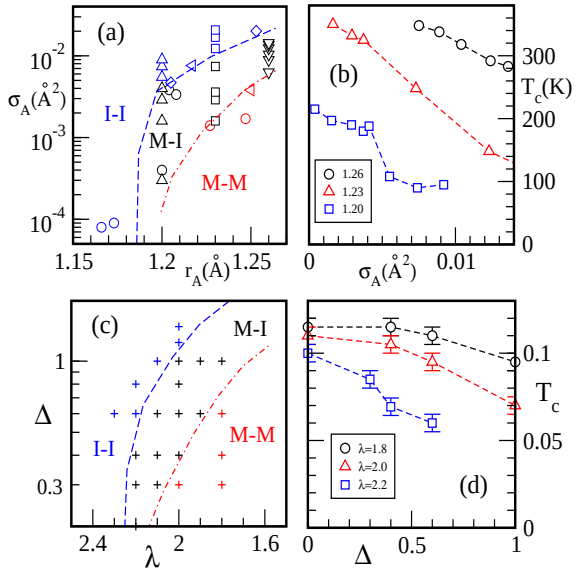

FIG. 3. Colour online: Transport regimes and ferromagnetic T_c: comparing data on the $x=0.3$ manganites with our $n=0.3$ results. (a). Transport 'phase diagram' indicating the nature of low T to high T crossover with changing r_A and σ_A, data from Ref[6-9] (b). $T_c(\sigma_A, r_A)$ in the manganites, from Ref[6-7], (c) transport crossovers from our calculation, and (d). our results on $T_c(\Delta,\lambda)$.

disorder on the electronic system. For a material of composition $A_{1-x}A'_xMnO_3$, say, r_A and σ_A depends on the radius of the A, A' ions as well as x. To disentangle the effect of varying carrier density (x) from that of varying 'coupling constants', there have been systematic studies of the manganites at fixed x, with controlled variation in r_A, related to our λ/t ratio, and σ_A, related to our Δ/t.

Focusing initially on $x=0.3$, the data from a wide variety of sources can be organised in terms of the transport response, $\rho(T)$, and magnetic T_c. We choose a simple characterisation where we construct the MIT phase diagram in terms of the low T to high T crossover observed in $\rho(T)$. For example, $La_{0.7}Sr_{0.3}MnO_3$ (LaSr), is a metal at both low T and $T>T_c$ so it shows M-M crossover. In that spirit LaCa shows M-I crossover, while PrCa is I-I. These simple 'binary' cationic systems are well studied, have relatively small σ_A, and the transport response can be argued to arise mainly from variations in r_A. However, more complex cationic combinations have been used, notably by Attfield and coworkers [6,7], to *vary* σ_A *at fixed* r_A *and* x. Our organisation of the experimental data, Fig.3.(a) uses three such families, at $r_A=1.26$, 1.23 and $1.20\mathring{A}$, as well as data from other sources [8,9] to highlight the combined impact of r_A and σ_A variation on transport character. We have used the 9 fold coordinated values of ionic radius from Shannon [17] in computing r_A and σ_A for about 30 compositions.

Four features are notable in the experimental MIT and T_c data, Fig.3.$(a)-(b)$, at $x=0.3$: (i) the 'clean' limit allows only a narrow window, $r_A\sim 1.18-1.20\mathring{A}$, for M-I

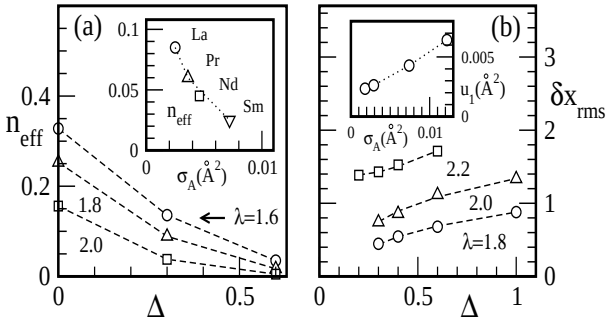

FIG. 4. (a) Computed optical spectral weight, n_{eff}, at cut-off $\omega = 0.5t$ and $T = 0.01$ for varying Δ and λ. Inset: data from Ref[10] on LaSr, *etc*, at $x = 0.4$, $\omega = 0.1$eV, plotted versus σ_A. The r_A values, LaSr downwards, are 1.256 $Å$, 1.232 $Å$, 1.22 $Å$ and 1.202 $Å$. (b) Our results on disorder induced lattice distortion at $T = 0.01$. Inset shows the σ_A induced increase in the mean square oxygen displacement at low T in a sequence of $x = 0.3$ and $r_A = 1.23Å$ manganites, from Ref[6].

crossover, (ii) the M-I region broadens with increasing σ_A at the cost of the M-M region (red/dot-dash line), disorder can *induce a thermally driven MIT*, (iii) at $T = 0$ just increasing σ_A can drive a metallic ground state insulating (blue/dashed line), (iv) the same σ_A has much stronger impact on transport and T_c at small r_A compared to large r_A, for example $\sigma_A \sim 0.01Å^2$ has only modest effect on T_c at $r_A = 1.26Å$, but leads to a large reduction at $r_A \lesssim 1.23Å$. While we cannot make a direct numerical correspondence between σ_A and Δ/t, etc, our results on transport crossovers, Fig.3.(c), and T_c, Fig.3.(d), show that *all the trends* $(i) - (iv)$ *above* are correctly reproduced. A fit to the detailed T dependence of resistivity will of course require a more sophisticated phonon model. Our $T_c^{max} \sim 0.12t \sim 300$K (for $t \sim 0.25$eV) compares reasonably with the maximum in Fig.3.(b).

Although the similarity of our results to experimental data on the manganites seems persuasive, let us examine how these results may be modified in a more realistic model. (i) The manganites involve *two e_g orbitals* coupled to *Jahn-Teller* (JT) phonons, with the possibility of orbital order. Our preliminary calculations with the 2 band JT model in 2D [18] suggests that for $x \sim 0.3 - 0.4$ there is no non trivial orbital order and the transport response is similar to what we observe here. The one band model does not capture the correct physics as $x \to 0$, or $x = 0.5$, but appears reasonable for $x \sim 0.3 - 0.4$. (ii) The oxygen atoms are corner shared among MnO_6 octahedra so the *phonon variables are cooperative*. We have not explored this aspect but believe the main effects would be lower critical EP coupling for localisation [12] and possibly a sharper MIT across T_c. (iii) There are *AF interactions* present in the manganites. We repeated the d-H-DE calculation in the presence of AF coupling and discovered that it leads to a sharper drop in T_c, shifts the MIT phase boundaries somewhat, and leads to an AF-I phase at large λ or Δ. The qualitative results of this paper, however, remain unaffected.

Finally, if our argument about disorder induced polaron formation is correct then the following features should be experimentally observed with increasing σ_A: (a) systematic suppression of low frequency optical spectral weight, n_{eff} at $\omega \lesssim 0.1$eV, at low T, (b) increase in the incoherent lattice distortion (oxygen Debye-Waller factor), progressively larger at smaller r_A, and (c) appearance of an increasingly deeper pseudogap in the tunneling DOS at low T. Fig.2 and Fig.4 quantify these effects. Experiments in the recent past do claim disorder induced polaron formation in $La_{0.54}Ba_{0.46}MnO_3$ [19] but more direct confirmation for $x \sim 0.3$ is desirable.

To conclude, we have studied a model with Holstein phonons, double exchange and quenched disorder, and illustrated the disorder enhancement of polaronic tendency and its interplay with spin fluctuations. Our results compare well with the disorder dependence of transport and T_c observed in the 'optimally doped' manganites. We make three testable predictions regarding the behaviour of optical spectral weight, oxygen Debye-Waller factor and tunneling density of states for controlled variations of σ_A in these materials.

We thank HRI for use of the Beowulf cluster and Saurabh Madaan for analysis of the experimental data.

* Present address: Institute for Physics, Theoretical Physics III, Electronic Correlations and Magnetism, University of Augsburg, 86135 Augsburg, Germany.

[1] See, *e.g*, *Colossal Magnetoresistive Oxides*, edited by Y. Tokura, Gordon and Breach, Amsterdam (2000).
[2] A. Moreo, *et al.* Phys. Rev. Lett. **84**, 5568 (2000).
[3] Y. Motome, *et al.*, Phys. Rev. Lett. **91**, 167204 (2003).
[4] D. Akahoshi, *et al.*, Phys. Rev. Lett. **90**, 177203 (2003).
[5] M. Uehara, *et al.*, Nature, **399**, 560 (1999), M. Fath, *et al.*, Science, **285**, 1540 (1999).
[6] L. M. Rodriguez-Martinez and J. P. Attfield, Phys. Rev. **B 58**, 2426 (1998), Phys. Rev. **B 54**, 15622 (1996), Phys. Rev. **B 63**, 024424 (2000).
[7] J. P. Attfield, Int. J. Inorg. Mat. **3**, 1147 (2001).
[8] G. L. Liu, *et al.*, Phys. Rev. **B 70**, 224421 (2004).
[9] J. M. D. Coey, *et al.*, Phys. Rev. Lett. **75**, 3910 (1995).
[10] E. Saitoh, *et al.*, Phys. Rev. **B 60**, 10362 (1999).
[11] H. Roder *et al.*, Phys. Rev. Lett. **76**, 1356 (1996).
[12] J. A. Verges, *et al.*, Phys. Rev. Lett. **88**, 136401 (2002).
[13] S. Yunoki, *et al.*, Phys. Rev. Lett. **81**, 5612 (1998).
[14] S. Kumar and P. Majumdar, cond-mat 0406082.
[15] S. Kumar and P. Majumdar, EPJ. **B 46**, 315 (2005).
[16] S. Kumar and P. Majumdar, Phys. Rev. Lett. **94**, 136601 (2005).
[17] R. D. Shannon, Acta. Cryst. **A 32**, 751 (1976).
[18] S. Kumar, A. P. Kampf and P. Majumdar, unpublished.
[19] T. J. Sato, *et al.*, Phys. Rev. Lett. **93**, 267204 (2004).